CARTILAGE AND BONE NEOFORMATION IN RABBIT CAROTID BIFURCATION ANEURYSMS AFTER ENDOVASCULAR COIL EMBOLIZATION

H. Plenk Jr.[-1], J.C. Shum[2], G.M. Cruise[2], M. Killer[3]

[1] Institute for Histology & Embryology, Bone & Biomaterials Research, Medical University of Vienna, A-1090 Vienna, Austria

[2]MicroVention Terumo, Aliso Viejo, CA 92656, USA

[3]Department of Neurology/Neuroscience Institute, Paracelsus Medical University, Christian Doppler Clinic, A-5020 Salzburg, Austria

Abstract

Occurrence and histomorphology of cartilage and bone neoformations was retrospectively evaluated in rabbit experimental aneurysms after endovascular coil embolization. During product development, 115 carotid bifurcation aneurysms were treated with hydrogel-containing devices (Hydro*Coil*®, n=77; Hydro*Soft*®, n=28; prototype Hydrogel-only, n=10; MicroVentionTerumo, Aliso Viejo, CA). Additional 29 aneurysms were treated with standard (n=22) or with degradable polymer-covered (n=7) platinum coils. After 4 to 52 weeks, the retrieved aneurysms were methylmethacrylate embedded, and ground sections were surface-stained with Rapid Bone Stain and Giemsa solution. Cartilage and/or bone tissue was assessed by light microscopy; respective tissue areas in the aneurysms were determined by computerized histomorphometry. Cartilage neoformation was observed from 26 to 52 weeks. Single chondrocytes to hyaline or fibrous cartilage areas, occupying up to 29% of the aneurysm cavity, were found in 6 aneurysms, treated with Hydro*Coil* (n=4), Hydrogel-only (n=1), and resorbable polymer (n=1) devices. Chondral ossification associated cartilage neoformation in 2 of these 4 Hydro*Coil*-treated aneurysms. Membranous woven and lamellar bone ossicles were observed from 13 to 52 weeks in 7 aneurysms, treated with Hydro*Coil* (n=3) and platinum coil (n=4) devices. Altogether, cartilage and/or bone neoformation was observed in 13 (9%) of 144 rabbit bifurcation aneurysms treated with various embolic devices. Incidence was low until 26 weeks, but increased at 52 weeks in both, Hydro*Coil* and standard platinum coil treated aneurysms. As the neoformations were predominantly located in proximity to the aneurysm neck, they could be related to the long-term mechanobiology of cell differentiation during fibrovascular healing of blood flow-exposed embolized aneurysms.

Keywords: metaplasias, cartilage, bone, coil embolization, carotid bifurcation aneurysms, rabbits.

*Address for correspondence:
H. Plenk
Institute for Histology & Embryology
Bone & Biomaterials Research
Medical University of Vienna
Schwarzspanierstrasse 17
A-1090 Vienna, Austria
Telephone Number: +43-1-4277-61336
FAX Number: +43-1-4277-61350
E-mail: hanns.plenk@meduniwien.ac.at

Introduction

Endovascular embolization therapy is a viable alternative to neurosurgical clipping for the treatment of human intracranial aneurysms (Molyneux *et al.*, 2005). With this technique, a microcatheter is inserted into the aneurysm sac under fluoroscopic guidance and detachable embolic devices, mainly platinum coils, are deployed into the aneurysm sac. Once the device is positioned satisfactorily, it is detached and the delivery pusher is removed. Generally, multiple devices are used to occlude the aneurysm sac.

The embolic devices filling the aneurysm sac induce blood stasis, leading to thrombosis. The desired thrombus organization into fibrous connective tissue can effectively isolate and strengthen the vulnerable aneurysm wall from the vasculature and thus prevent (re)rupture. However, optimal angiographic occlusion and thrombus organization inside human aneurysm sacs is not inevitable (Bavinzski *et al.*, 1999), particularly in larger aneurysms. This led to the development, pre-clinical testing, and clinical use of embolic devices combining the original platinum coils with expandable hydrogels (Kallmes and Fujiwara, 2002; Arthur *et al.*, 2005; Ding *et al.*, 2005), or degradable polymers (Murayama *et al.*, 2003; Linfante *et al.*, 2005; Bendszus and Solymosi, 2006). Furthermore, attachment of proteins (Murayama *et al.*, 1997), growth factors (de Gast *et al.*, 2001), or autologous fibroblasts (Kwon *et al.*, 2003) to embolic devices have also been evaluated in experimental aneurysms.

While in most cases thrombus organization results in a more or less vascularized fibrous connective tissue, in some experimental aneurysms cartilage and/or bone metaplasias were observed. Previously, incidental observation of chondrocytes and hyaline cartilage, but also only metachromatic matrix, was reported in five of twelve (42%) rabbit bifurcation aneurysms treated with Hydro*Coil*® (MicroVention Terumo, Aliso Viejo, CA, USA) devices after twelve months post-embolization follow-up (Killer *et al.*, 2004). More recently, bone metaplasia inside the aneurysm sac was found in two of seventy-one (3%) rabbit elastase aneurysms at 3 and 12 months after treatment with platinum coils (Dai *et al.*, 2007). Furthermore, bone formations were observed in a human intracranial aneurysm retrieved about 6 years after treatment with platinum coils (Plenk, unpublished observation).

Based on these reports, a retrospective evaluation was performed for the occurrence and histomorphology of cartilage and/or bone in the histological sections of 144 rabbit carotid bifurcation aneurysms from product development studies of embolic devices.

Materials and Methods

Embolic Devices

Hydro*Coil*® devices (MicroVention Terumo), both prototypes and commercially available products (Hydro*Coil* 10, Hydro*Coil* 14, and Hydro*Coil* 18) were used to embolize 77 aneurysms. The prototype devices consisted of an inner layer of platinum coil and an outer layer of dried hydrogel (poly(acrylamide-co-acrylic acid). A stretched platinum coil was placed over the dried hydrogel on the commercially available devices.

Hydro*Soft*® devices (MicroVention Terumo), both prototypes and commercially available product, were used to embolize 28 aneurysms. These devices consist of an outer layer of stretched platinum coil and an inner layer of hydrogel (poly (poly(ethylene glycol)-co-acrylic acid).

Prototype Hydrogel-only embolic devices (MicroVention Terumo) were used to embolize 10 aneurysms. These devices consist of a hydrogel prepared from an acrylated poly(ether) rendered radiopaque with an acrylated tri-iodo aromatic compound or barium sulphate (Constant *et al.,* 2008).

Commercially available platinum coils (MicroPlex Coiling System®, MicroVention Terumo, and Guglielmi Detachable Coils®, Boston Scientific), were used exclusively in 22 aneurysms, but also in combination with Hydro*Coil* and Hydro*Soft* devices.

Commercially available Matrix® devices (Boston Scientific, Fremont, CA) were used to embolize 7 aneurysms. These devices consist of a biodegradable outer poly (glycolic acid-co-lactic acid) layer and an inner platinum coil.

After polymerization, all the hydrogels were washed in copious distilled water to remove the sodium chloride particles used for creating the porosity. All platinum coils were heat treated to conserve their secondary shapes, and clean washed in isopropyl alcohol or ethanol. All the manufacturing steps shown in Figure 1 are performed under clean room conditions. The assembled devices were gamma or ethylene oxide sterilized.

Experimental procedures

All studies had been carried out in accordance with Austrian regulations on animal experiments and were approved by the Austrian Federal Ministry for Education, Science, and Culture (GZ 68.210/1 and 66.012/17).

For all operative procedures (aneurysm creation, embolization, and angiographies), the rabbits were pre-anesthetized with an intramuscular injection of ketamine (20-30 mg/kg) and 2% xylazine (0.2 ml). Anaesthesia was maintained with intravenous injections of ketamine:xylazine:saline (5:1:5, 0.5-1 ml/kg/hr). For post-operative pain control, Meloxicam (0.2 mg/kg subcutaneously for 5 days) was administered. The animals were kept in single cages with pellet food and water *ad libitum*.

Microsurgical aneurysm creation

Carotid bifurcation aneurysms (schematic drawing in Fig. 2a) were microsurgically created in 144 New Zealand white rabbits (3-4 kg body weight) according to established methods (Forrest and O'Reilly, 1989). Briefly, both common carotid arteries were exposed and clamped distally and proximally. A bifurcation was created by an end-to-side anastomosis of the left to the right common carotid artery. A portion of the jugular vein, resected between ligatures, was sutured to the carotid artery junction to serve as an aneurysm sac. All vascular suturing was performed with non-resorbable Prolene® suture. The clamps were released and haemostasis was assured. The skin incision was closed using a multi-layer subcutaneous technique with degradable Vicryl® suture. At least three weeks passed after aneurysm creation before embolization occurred.

Aneurysm embolization, treatment groups, and follow-up

At the time of aneurysm embolization, the right femoral artery was exposed, ligated distally, and a small arteriotomy was made. A 5Fr guide catheter was inserted through the arteriotomy and advanced to the right common carotid artery. Performing a digital subtraction angiography (DSA) by perfusion with contrast medium, the size and shape of the created aneurysm was assessed, using an US-dime (Ø 17.8 mm) for radiograph calibration (Fig. 2b). Upon satisfactory placement of the guide catheter 500U heparin were administered intravenously. A two-marker microcatheter, typically an Excel 14 or Excelsior SL-10 (Boston Scientific), was advanced through the guide catheter and into the aneurysm sac.

As in clinical application, multiple devices were utilized to fill the aneurysm sac. In the Hydro*Coil* and Hydro*Soft* groups, one or two platinum coils with a complex or 3D shape were deployed first to frame the aneurysm sac. The endpoint of the embolization was angiographic occlusion. Post-treatment angiography (DSA) was performed to document occlusion, the shape of the embolic mass, and flow through the parent arteries (Fig. 2c). All catheters were removed and the femoral artery was ligated proximal to the arteriotomy. The skin incision was closed using a multi-layer subcutaneous technique with Vicryl® suture. The five treatment groups and follow-up durations are summarized in Table 1. At follow-up, final angiography (DSA) was performed as described above. Angiographies of one experimental aneurysm before embolization, after embolization, and at follow-up are shown in Figures 2b-d. The rabbits were euthanized with an intravenous injection of Embutramid-Tetracain solution (1 ml/4.5 kg). The aneurysm and parent arteries were excised and placed in 10% neutral buffered formalin.

Histologic processing

After immersion fixation in 10% neutral buffered formalin for several days, the aneurysms containing metals
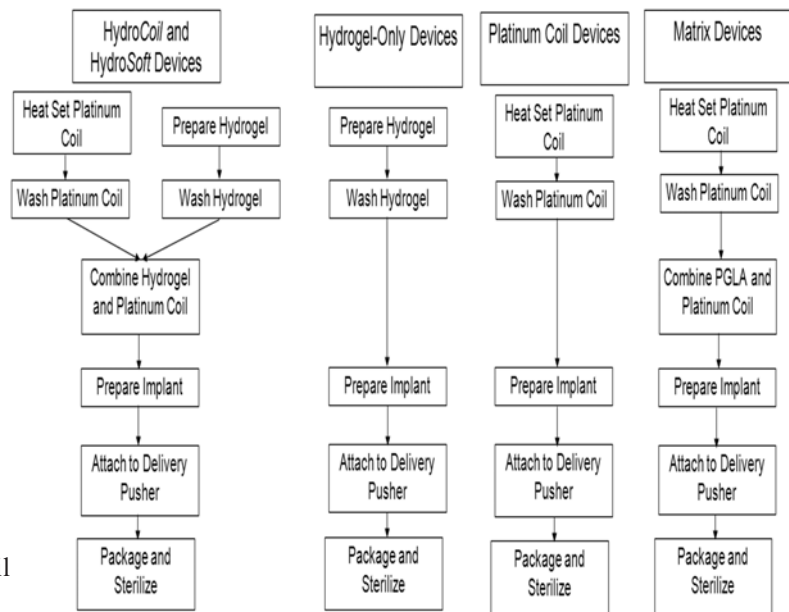
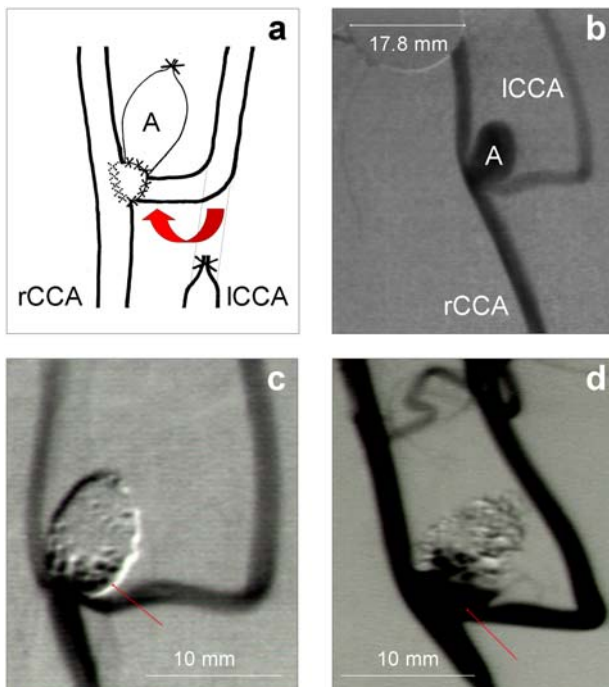**Figure 1.** Flow chart diagram of the coil manufacturing steps.

Figure 2. **(a)** Schematic drawing of the microsurgical creation of a carotid bifurcation aneurysm (A) by suturing (x = sutures) a segment of the jugular vein onto the end-to-side anastomosis of the left common carotid artery (lCCA) to the right common carotid artery (rCCA). **(b)** Pre-embolization digital subtraction angiogram (DSA) of Rabbit 50 carotid bifurcation aneurysm (A) with calibration tool. **(c)** Post-embolization DSA, showing dense packing of the platinum and HydroCoil® embolization devices in sac and dome of the aneurysm, but loose coil loops with some contrast medium perfusion at the orfice (red arrow). **(d)** Pre-sacrifice DSA, 52 weeks post-embolization, showing increased contrast medium perfusion of orifice and adjacent sac of the aneurysm (red arrow).

Table 1: Numbers of Re-evaluated Aneurysms per Treatment Group, Follow-up Periods, and Incidence of Cartilage/Bone Metaplasias

Treatment group (n = aneurysms)	Follow-up periods					
	4 wks	8 wks	13 wks	26 wks	39 wks	52 wks
Hydro*Coil* (n=77)	18	3	4 **1B**	24 **1B**	16	12 **2C, 1B, 2C&B**
Hydro*Soft* (n=28)	19	--	--	9	--	--
Hydrogel-only (n=10)	3	--	--	7 **1C**	--	--
Platinum Coils (n=22)	6	--	1	8 **1B**	--	7 **3B**
Matrix Coils (n=7)	--	--	--	--	7 **1C**	--

C…Cartilage   **B…**Bone   **C&B…**Cartilage&Bone

(Hydro*Coil*, Hydro*Soft*, platinum coil, and Matrix devices) were dehydrated in a graded series of ethanol and embedded in methyl methacrylate according to a standard protocol (Plenk, 1986). After polymerization, consecutive longitudinal thick sections of the aneurysms were obtained with a circular diamond saw (ISOMET®, Buehler Ltd., Lake Bluff, IL) and ground to a thickness of 60-80 microns using the EXAKT® system (EXAKT Apparate Bau GmbH, Norderstedt, Germany). The polished ground sections were routinely surface stained with Sanderson's Rapid Bone Stain (SURGIPATH Medical Inc., Richmond, VA, USA) without acid-fuchsin counterstain, or with toluidine blue-basic fuchsin. Surface staining with Giemsa solution (Merck AG, Darmstadt, Germany) and Krutsay calcium salt stain (for details see Plenk, 1986) were used on repolished ground sections when bone formations were observed.

As the prototype hydrogel-only embolic-treated aneurysms did not contain metal, microtome sections were prepared. Three aneurysms were immersed in OCT® (Ted Pella, Redding, CA), bisected longitudinally through the neck of the aneurysm, and solidified in liquid nitrogen-cooled isopentane to cut 10 micron thick frozen sections (Leitz KRYOSTAT 1720, Leica Microsystems, Vienna, Austria). Seven aneurysms were embedded in methyl methacrylate as above and sawed longitudinally through the neck of the aneurysm. Five-micron thick sections were prepared using a rotary microtome (Jung AUTOCUT 1041, Leica Microsystems, Vienna, Austria). The frozen or plastic-embedded microtome sections were stained with haematoxylin & eosin and Movat pentachrome stains.

All ground and microtome sections were evaluated using light microscopy. Cartilage and bone tissues were identified morphologically. Immunohistochemical staining of cells and extracellular matrix components could not be performed due to the methyl methacrylate embedding mainly utilized in this study.

Histometric quantification

At least two ground sections from aneurysms with cartilage and bone metaplasias underwent computerized morphometry quantification (Sherif *et al.*, 2006; Cruise *et al.*, 2007). The ground sections were photographed using an AxioCam MRc5 digital camera mounted on an AxioImager A1 microscope with a 1.25X objective and analyzed using AxioVision 4.6 software (Carl Zeiss Microimaging, Thornwood, NY, USA). The aneurysm area, occluded area, and cartilage and/or bone areas were quantified.

Statistical analyses

Due to the small or inconsistent numbers of aneurysms available for evaluation in the treatment groups and follow-up periods, no statistical analyses were performed.

Results

All rabbits survived to follow-up without any clinical signs of morbidity or mortality. Depending on follow-up periods,
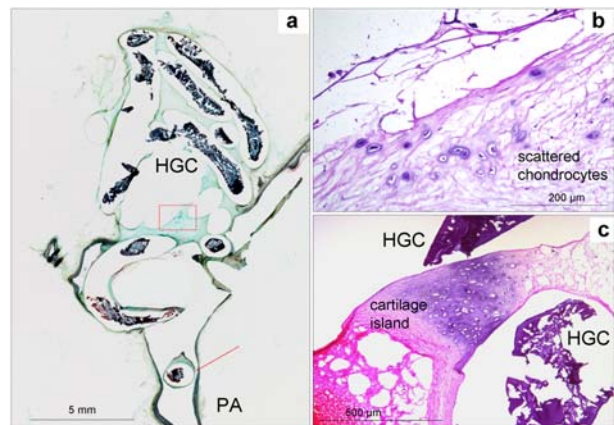

Figure 3. Microtome frozen section of the Rabbit 76 aneurysm, 26 weeks post-embolization with Hydrogel-only devices. **(a)** Overview (Movat stain), showing partly empty coil tracks and shrinkage artifacts of the dehydrated hydrodrogel coils (HGC). A neointima-covered coil (red arrow) can be seen in the parent artery (PA). **(b)** Enlarged rectangle (H&E stain) in a), showing scattered chondrocytes in the loose connective tissue between the coil tracks. **(c)** A fibrocartilage island with typical basophilic staining of the extracellular matrix (H&E stain) can be seen between the hydrogel coils (HGC) in a consecutive section.

different stages of thrombus organization with a more or less fibrous and vascularised connective tissue were found in the aneurysms of all treatment groups. Single or multiple macrophages and multinucleated foreign body giant cells were found at implant-tissue interfaces. Cartilage, bone, or cartilage/bone metaplasias were observed in six, three, and two aneurysms, respectively.

At 26 weeks, in the aneurysm sac of rabbit 76 (Fig. 3a) cartilage metaplasia with scattered chondrocytes (Fig. 3b) and fibrous cartilage islands with typical basophilic staining of the extracellular matrix (Fig. 3c) was observed in the loose connective tissue between the Hydrogel-only embolic devices.

At 39 weeks, only in one of two ground sections of the aneurysm sac of rabbit 160 treated with Matrix devices showed a small island of fibrocartilage in the more fibrous connective tissue filling the aneurysm sac. Only few foreign body cells and no remnants of the degradable polymer covering the coils were observed around these devices.

At 52 weeks, four aneurysms treated with Hydro*Coil* devices showed cartilage neoformation. In only one of five consecutive ground sections of Rabbit 60, a single hyaline cartilage island was observed between the coils. In one of three ground sections of Rabbit 63, some scattered cells, resembling chondrocytes, within a dense matrix showing metachromasia after RBS (Rapid Bone Stain) staining were observed. In addition, a small cartilage island was found in the wall of the carotid artery just adjacent to one of the sutures from aneurysm creation and a branching artery. Instead of smooth muscle cells, rounded cells resembling chondrocytes were lying between the elastic membranes of the arterial wall and were embedded in a metachromatic

Table 2: Histometric data summary of aneurysms showing cartilage and/or bone metaplasia

Rabbit number, Treatment group, Follow-up duration	Slide	Aneurysm area (mm^2)	Occluded area (%)	Cartilage area (%)	Bone area (%)
Rabbit 76 Hydrogel-only 26 weeks	1	60.4	100	**1.0**	0.0
	2	57.8	100	**0.1**	0.0
Rabbit 160 Matrix 39 weeks	1	7.9	78	0.0	0.0
	2	6.2	87	**3.0**	0.0
Rabbit 39 HydroCoil 13 weeks	1	32.5	99	0.0	**2.1**
	2	29.9	94	0.0	0.0
Rabbit 37 HydroCoil 26 weeks	1	45.6	87	0.0	0.0
	2	52.3	84	0.0	**0.2**
Rabbit 50 HydroCoil 52 weeks	1	53.8	58	**6.8**	**0.7**
	2	60.8	62	**6.0**	**0.3**
	3	61.1	85	**19.7**	**0.8**
	4	63.8	90	**17.6**	**0.8**
	5	61.3	94	**28.7**	**1.5**
Rabbit 59 HydroCoil 52 weeks	1	7.1	100	0.0	0.0
	2	9.1	100	0.0	**1.2**
Rabbit 60 HydroCoil 52 weeks	1	9.8	100	0.0	0.0
	2	19.1	94	0.0	0.0
	3	20.1	86	**0.5**	0.0
	4	20.7	68	**1.9**	0.0
	5	16.4	77	0.0	0.0
Rabbit 63 HydroCoil 52 weeks	1	35.8	97	0.0	0.0
	2	35.1	99	**0.4**	0.0
	3	28.9	100	0.0	0.0
Rabbit 67 HydroCoil 52 weeks	1	25.9	82	0.0	0.0
	2	23.5	98	**1.0**	**1.1**
Rabbit 47 Pt Coil 26 weeks	1	14.1	84	0.0	**2.1**
	2	12.6	88	0.0	**3.9**
Rabbit 81 Pt Coil 52 weeks	1	63.5	100	0.0	**8.6**
	2	89.6	100	0.0	**9.3**
Rabbit 82 Pt Coil 52 weeks	1	85.9	89	0.0	**2.2**
	2	89.4	81	0.0	**1.4**
Rabbit 86 Pt Coil 52 weeks	1	43.9	97	0.0	0.0
	2	45.5	94	0.0	**0.4**

matrix. In one of two ground sections of Rabbit 67, smaller hyaline cartilage areas and endochondral bone formation were observed between the hydrogel coated coils. The basophilic vacuolated swollen hydrogel with rounded cells in the voids was often difficult to distinguish from cartilage tissue.

In all 5 ground sections of Rabbit 50, large areas of hyaline cartilage were found between the coils, along the neointima/new vessel wall (Figs. 4 and 5), and in the aneurysm sac, making up to 29% of the aneurysm area (Table 2). Cartilage formation had occurred in direct contact with the outer interface of the swollen hydrogel, as well as within gaps between the hydrogel coating and the inner platinum coils. Again, the basophilic staining of the swollen vacuolated hydrogel was sometimes difficult to distinguish from cartilage matrix, but rounded cells occupying these vacuoles definitely resembled chondrocytes surrounded by matrix (Fig. 5b). Larger cartilage areas showed membranous bone formation at the surface (Figs. 5c-d), and also endochondral bone formation with marrow cavities, containing fatty and hematopoietic marrow (Figs. 5e-f). Mineralization of bone and hypertrophic cartilage matrix (Fig. 5d) was proven by the calcium salt staining.
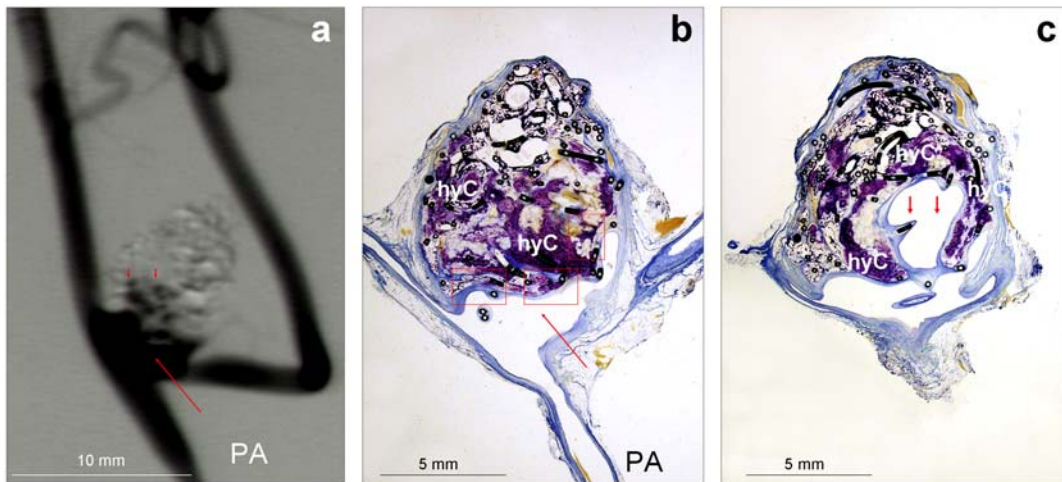
Figure 4. (a) Pre-sacrifice DSA of Rabbit 50, 52 weeks post-embolization, showing dense contrast medium perfusion of the parent arteries (PA), the orifice (red arrow) and the adjacent sac of the aneurysm (red arrow-heads). **(b)** and **(c)** Overviews of corresponding consecutive ground sections (Giemsa stain) of the aneurysm, showing an empty vascular space at the orifice (red arrow in b), and its expansion into the adjacent sac (red arrow-heads in(c). A big mass of violet-stained hyaline cartilage (hyC) can be seen in the centre of the sac, and surrounding the vascular space.
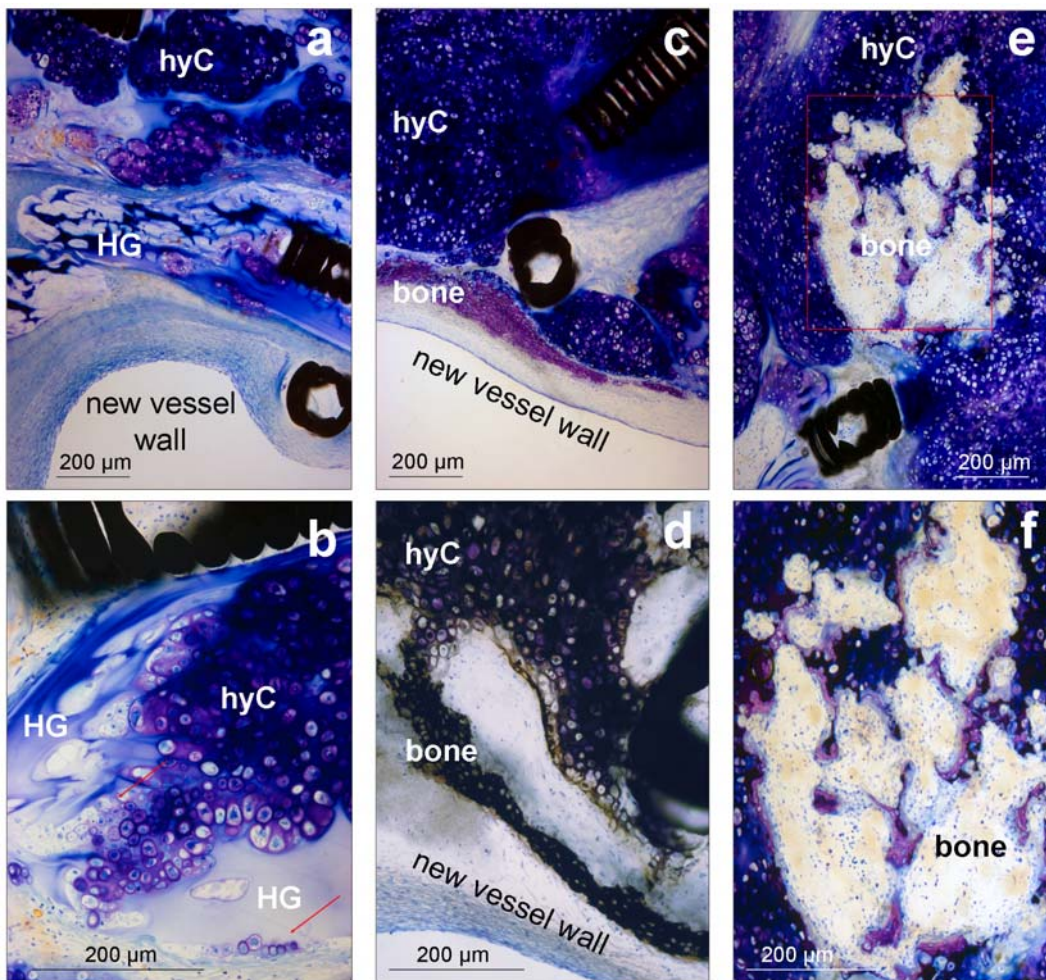

Figure 5. Enlarged rectangles (Giemsa stain, (d) Krutsay stain) of Figure 3b. **(a)** Hyaline cartilage (hyC) had been formed between and within the hydrogel (HG) of the coils underneath the new vessel wall covering the orifice. **(b)** Hyaline cartilage and groups of chondrocytes with basophilic and pink-stained extracellular matrix on the surface and within the vacuoles of the swollen basophilic hydrogel (HG). **(c)** Purple-stained membranous bone was formed on the surface of hyaline cartilage (hyC) surrounding the new vessel wall. **(d)** After re-polishing, the Krutsay calcium-salt stain shows black silver precipitation on mineralized bone and cartilage (hyC). **(e)** Endochondral bone formation and marrow cavities (red rectangle) within hyaline cartilage (hyC). **(f)** Enlarged rectangle shows active formation of purple-stained endochondral bone trabeculae around basophilic mineralized cartilage remnants and hypertrophic chondrocytes.
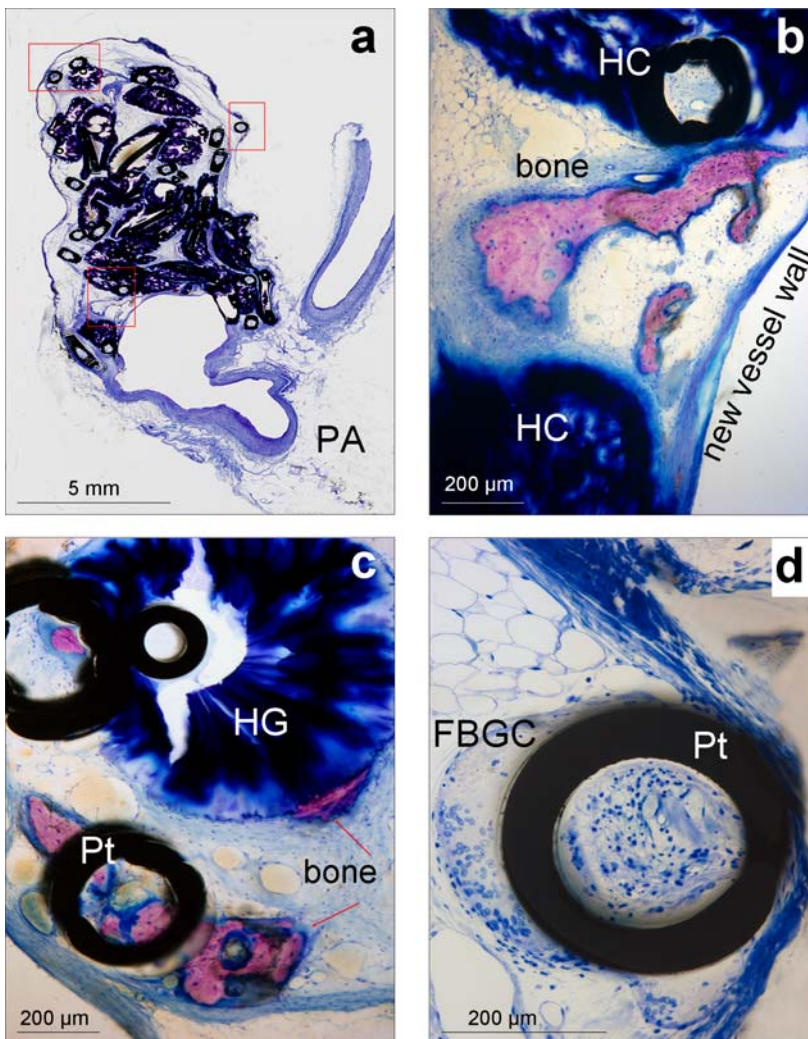
Figure 6. **(a)** Ground section overview (Rapid Bone Stain) of the Rabbit 37 aneurysm, 26 weeks post-embolization. Enlarged rectangles of Figure 5a (Giemsa stain after re-polishing), **(b)** showing a large purple-stained ossicle between the HydroCoils (HC) underneath the new vessel wall of the orifice, **(c)** Small ossicles (red arrows) near the aneurysm wall of the dome, formed in direct contact with the hydrogel (HG) and the surface and lumen of bare platinum coils (Pt). **(d)** The foreign body giant cell (FBGC) response to bare platinum coils (Pt) is much more pronounced than to hydrogel-coated coils.

Three aneurysms treated with Hydro*Coil* devices showed solely membranous bone neoformation. At 13 weeks, woven and lamellar bone ossicles were found mainly along the aneurysm wall in 1 of 2 ground sections of the aneurysm from Rabbit 39. At 26 weeks, membranous bone formations were also observed in 2 of 3 ground sections prepared from the aneurysm of Rabbit 37 (Fig. 6a). One larger ossicle was found underneath the neointima/new vessel wall covering the orifice (Fig. 6b), and several small ossicles were observed along the aneurysm wall near the aneurysm dome (Fig. 6c). The ossicles consisted of woven and lamellar bone with signs of previous remodelling, and showed active bone formation. The ossicles along the aneurysm wall were in direct contact with platinum coils and with the hydrogel of the Hydro*Coil* devices. Bone could be seen also within the lumen of the platinum coils, despite the prominent foreign body cell response at these interfaces (Fig. 6d).

At 52 weeks, the small, wide-necked aneurysm originally treated with Hydro*Coil* devices was found empty, and the embolic devices formed an occluding embolus trapped in a parent artery. Small woven bone ossicles and larger sinusoidal vessels were observed between the tightly packed hydrogel-coated coils.

Four aneurysms treated with standard platinum coils also showed membranous bone neoformation. At 26 weeks,

woven bone with lamellar compaction was found scattered throughout the neck region, even inside the platinum coils, in both ground sections of the aneurysm from Rabbit 47. At 52 weeks, woven and lamellar bone was found throughout the aneurysm sac, neck, and within a coil protrusion into parent arteries in both ground sections of the aneurysm from Rabbit 81. Woven bone islands with some lamellar bone, and containing fatty and red marrow, were localized in the dome of the aneurysm sac near a large recanalization in both ground sections of the aneurysm from Rabbit 82. Small woven bone islands behind the neck of the aneurysm were present in one of two ground sections of the aneurysm from Rabbit 86.

The histometric results of all the histological sections with cartilage and/or bone formation are summarised in Table 2.

As summarised in Table 1, neoformation of either scattered chondrocytes or islands of more fibrous cartilage was observed in one aneurysm embolized with prototype Hydrogel-only embolic devices, in one embolized with Matrix devices, and in two aneurysms embolized with Hydro*Coil* devices. Hyaline cartilage together with endochondral bone formation was observed in two aneurysms treated with Hydro*Coil* devices. Membranous bone formation was observed in three aneurysms treated with Hydro*Coil* devices, and in four aneurysms treated

with platinum coils. Overall, the incidence of cartilage or bone neoformation was approximately 4.1% (6 of 144) and 6.3% (9 of 144), respectively. The combined incidence of cartilage and/or bone metaplasia in the treatment group Hydro*Coil* was about 9% (7 of 77), Hydro*Soft* 0% (0 of 28), prototype Hydrogel-only embolic 10% (1 of 10), platinum coil 18% (4 of 22), and Matrix 14% (1 of 7). Related to follow-up periods (Table 1), up to 26 weeks post-embolization cartilage metaplasia was only observed at 26 weeks in one aneurysm (1% of 102), while bone metaplasia was observed at 13 and 26 weeks in 3 (2.9% of 102) aneurysms. At follow-up durations longer than 26 weeks, cartilage neoformation was observed in about 11.9% (5 of 42), and bone neoformation in about 14.3% (6 of 42) of the aneurysms.

Discussion

In this study, cartilage and bone neoformations are described in aneurysm sacs and parent arteries of rabbit bifurcation aneurysms after endovascular embolization. In order to understand the pathomechanism of these tissue metaplasias during fibro-vascular thrombus organization, several explanations and influences have to be considered. Cartilage metaplasia, calcification and ectopic bone formation have been observed in vascular tissues besides aneurysms. Ectopic cartilage in the arterial media has been demonstrated in conjunction with transduction of an adenoviral vector expressing an active form of transforming growth factor-β1 (TGF- β1) in rats (Schulick *et al.*, 1998), in the aortae of atherosclerotic mice (Qiao *et al.*, 1995), and in human heart valves (Seemayer *et al.*, 1973). On the other hand, in the aortae of mice lacking matrix GLA protein calcifications were found (Luo *et al.*, 1997). In human atherosclerosis, dystrophic calcifications are common which can be transformed into heterotopic bone formations (Cotran *et al.*, 1989).

Complementing the earlier incidental observations (Killer *et al.*, 2004), the present study is the first report of cartilage neoformation in experimental aneurysms. Overall, the incidence of smaller or larger cartilage neoformations was approximately 4.2% (6 of 144), occupying at 52 weeks up to 29% of one aneurysm area (Table 2). The incidence of bone neoformations in the present study was 6.3% (9 of 144), thus incidence is greater than in the only other study (Dai *et al.*, 2007) reporting bone metaplasias in 3% (2 of 71) rabbit elastase aneurysms after similar durations, 12 and 52 weeks after embolization with platinum coils.

These incidences are probably lower than in reality since, in most cases, the cartilage and bone formations occupied small percentages of the aneurysm area, and the histological processing techniques result in only small portions of the aneurysm volume for evaluation. For example, from 500 micron thick tissue slices (wavering blade loss added) through the aneurysm sac about 80 micron thick ground sections are prepared, and only about 5 microns of surface-stained tissue can be evaluated under the microscope for the presence of cartilage or bone neoformations.

In the present re-evaluation, one major influence on the incidence of both these metaplasias is the length of time between embolization and follow-up. While metaplasias were found only in single aneurysms until 26 weeks, they were definitely more prevalent at 52 weeks. Neoformation of bone was first observed at 13 weeks, and of cartilage at 26 weeks post-embolization. At 52 weeks follow-up duration, the incidence of cartilage (11.9%) and bone (14.3%) formation in 21.4% (9 of 42) aneurysms was greater than in those with follow-ups of 26 weeks or less (3.9%, 4 of 102). Because preclinical studies in product development were usually terminated at 26 weeks, some study protocols lacked longer durations. Long-term effects such as aneurysm recanalization have so far been studied up to 52 weeks after Hydro*Coil* and standard platinum coil embolization. This apparent lack of long-term follow-up may partially explain why cartilage and/or bone neoformation was not observed in the aneurysms treated with Hydro*Soft* devices (Table 1).

Animal species and type of experimental aneurysm model are apparently other influences on this metaplastic tissue differentiation during thrombus organization. In previous studies using the sidewall model in canines (Mawad *et al.*, 1995), pigs (Pile-Spellman and Wu, 1997), and primates (Tenjin *et al.*, 1995), or the carotid bifurcation model in rabbits (Reul *et al.*, 1997), no bone or cartilage metaplasias were reported. As mentioned above, bone metaplasia was observed in two of seventy-one rabbit elastase aneurysms treated with platinum coils (Dai *et al.*, 2007). Recently, the comparative histometric results of rabbit elastase, canine bifurcation, and canine sidewall experimental aneurysm embolization with Hydro*Coil* and platinum coil devices were reported (Cruise *et al.*, 2007). Bone metaplasia was also observed in the sac of one rabbit elastase bifurcation aneurysm six months after embolization with platinum coils out of a total of seventy rabbits. However, neither cartilage nor bone formation was observed in any of the fifty-nine canine bifurcation and the forty canine sidewall aneurysms, respectively. Together with the present results, cartilage and bone metaplasia in experimental aneurysms is more prevalent in the rabbit compared to the canine or other species. While these metaplasias were not observed in sidewall models, they were found in bifurcation models, in which the aneurysm is under continuous impact of pulsatile blood flow. Interestingly, bone neoformation was also observed in a human intracranial bifurcation aneurysm about 6 years after embolization with platinum coils (Plenk, unpublished observation).

Although cartilage metaplasia in the cardiovascular system has been reported in a number of locations and models (Luo *et al.*, 1997; Schulick *et al.*, 1998; Seemayer *et al.*, 1973), the pathogenesis of these metaplasias remains unclear. It has been postulated that metaplasias are a result of undifferentiated vascular cells present in the arterial wall (Watson *et al.*, 1994), and that arterial wall smooth muscle cells can differentiate into chondrocytes and osteoblasts (Schulick *et al.*, 1998). Our observation of a cartilage island in the media of the parent carotid artery would support both hypotheses.

Cartilage metaplasia was present in the media of rat arterial walls after treatment with an adenoviral vector expressing active TGF-β at four weeks, but not at one, two or eight weeks (Schulick *et al.*, 1998). This indicates that the response to increased concentrations of TGF-β1 takes some time to develop and is reversible once the high concentration of TGF-β1 subsides. Gene expression analysis after the embolization of porcine sidewall aneurysms with Matrix devices has shown that TGF-β1 is upregulated at three and seven days after embolization with this degradable protein-covered device (Lee *et al.*, 2007). Thus, early release of TGF-β1 and other cytokines and growth factors may induce cartilage and bone metaplasias in the cardiovascular environment, but it is not yet clear if this holds true for the present 39 weeks long-term observations in experimental aneurysms. However, the inflammatory process of thrombus organization itself may provide sufficient biochemical signals to initiate such a metaplastic differentiation (van Aken and Emeis, 1982, 1983).

Finally, differentiation of mesenchymal cells is also influenced by the biomechanical environment inside the aneurysm sac. Cartilage metaplasias were observed using the Hydro*Coil*, prototype hydrogel-only, and Matrix embolic devices, but not with the Hydro*Soft* and the platinum coil devices. This lack of cartilage metaplasia at least in the Hydro*Soft* group may only be related to shorter follow-up duration, as discussed above. However, the mode of action, and apparently also the histomorphology of the swollen hydrogels are both comparable with cartilage extracellular matrix. It is noteworthy that cartilaginous constructs have been grown *in vitro* in various polymer and hydrogel scaffolds (Rice and Anseth, 2004), and in bioreactors with (Freed *et al.*, 1998) and without (Marlovits *et al.*, 2003) scaffolds. Low shear stress rotating bioreactor vessels or application of multi-axial mechanical stimulation and oscillating hydrostatic pressure on cultures can simulate the *in vivo* mechanical loading that is essential for chondrocyte differentiation and cartilage extracellular matrix production (Waldman *et al.*, 2007). These loading conditions can be compared with the mechanobiology of tissue healing within the environment of bifurcation aneurysm models exposed to pulsatile blood flow. Cartilage formation, observed mainly after hydrogel containing devices, provides physical properties similar to the swollen hydrogel filling the aneurysm sac, resulting in more resistance to the blood flow impact and possibly reducing the risk of recanalization and (re)rupture. The chondral ossification and membranous bone formation, found mainly adjacent to the new vessel wall covering the aneurysm neck, may provide even increased resistance to blood flow impact. Interestingly, newly formed ossicles were in direct contact with the hydrogel surface, as well as with the platinum coils, despite the pronounced foreign body cell response to the latter material. Thus, the mechanical, but not the biological compatibility of the various embolic devices may have influenced this metaplastic cartilage and bone differentiation.

While cartilage and/or bone neoformation was found in 13 (9%) of 144 rabbit bifurcation aneurysms in the present evaluation, it does have limitations. It was a retrospective analysis of existing sections from previously conducted studies performed in the course of product development of hydrogel-platinum coil hybrid devices. As a result, the numbers of aneurysms and follow-up durations are not consistent between groups. Due to the use of standard methyl methacrylate embedding and surface-stained ground sections with the implants *in situ* in this study, cartilage and bone were only identified by histomorphology and staining properties, but immunohisto- and cytochemical staining to elucidate additional information about cell types and extracellular matrix was precluded.

Conclusions

Cartilage and bone metaplasias were observed in six (4.2%) and nine (6.3%) of 144 rabbit bifurcation aneurysms up to 52 weeks after embolization with a variety of embolic devices. Greater incidences of cartilage and bone metaplasia were observed in follow-up durations at least six months post-embolization. The mechanobiology inside the aneurysm sac, including the swollen hydrogel and thrombus organization under pulsatile blood flow, may have contributed to the neoformation of cartilage and/or bone in rabbits.

Acknowledgements

References

Arthur AS, Wilson SA, Dixit S, Barr JD (2005) Hydrogel-coated coils for the treatment of cerebral aneurysms: preliminary results. Neurosurg Focus **18**: E1.

Bavinzski G, Talazoglu V, Killer M, Richling B, Gruber A, Gross CE, Plenk H, Jr. (1999) Gross and microscopic histopathological findings in aneurysms of the human brain treated with Guglielmi detachable coils. J Neurosurg **91**: 284-293.

Bendszus M, Solymosi L (2006) Cerecyte coils in the treatment of intracranial aneurysms: a preliminary clinical study. Am J Neuroradiol **27**: 2053-2057.

Constant MJ, Keeley EM, Cruise GM (2008) Preparation, characterization, and evaluation of radiopaque hydrogel filaments for endovascular embolization. J Biomed Mater Res B Appl Biomater DOI: 10.1002/jbm.b.31217 (in press)

Cotran R, Kumar V, Robbins S (1989) Robbins Pathologic Basis of Disease, 4th ed. Philadelphia-London-Toronto-Tokyo, W.B. Saunders Company.

Cruise GM, Shum JC, Plenk H Jr. (2007) Hydrogel-coated and platinum coils for intracranial aneurysm

embolization compared in three experimental models using computerized angiographic and histologic morphometry. J Mater Chem **17**: 3965-3973.

Dai D, Ding YH, Kadirvel R, Lewis DA, Cloft HJ, Kallmes DF (2007) Bone formation in elastase-induced rabbit aneurysms embolized with platinum coils: report of 2 cases. Am J Neuroradiol **28**: 1176-1178.

de Gast AN, Altes TA, Marx WF, Do HM, Helm GA, Kallmes DF (2001) Transforming growth factor beta-coated platinum coils for endovascular treatment of aneurysms: an animal study. Neurosurgery **49**: 690-694; discussion 694-696.

Ding YH, Dai D, Lewis DA, Cloft HJ, Kallmes DF (2005) Angiographic and histologic analysis of experimental aneurysms embolized with platinum coils, Matrix, and HydroCoil. Am J Neuroradiol **26**: 1757-1763.

Forrest MD, O'Reilly GV (1989) Production of experimental aneurysms at a surgically created arterial bifurcation. Am J Neuroradiol **10**: 400-402.

Freed LE, Hollander AP, Martin I, Barry JR, Langer R, Vunjak-Novakovic G (1998) Chondrogenesis in a cell-polymer-bioreactor system. Exp Cell Res **240**: 58-65.

Kallmes DF, Fujiwara NH (2002) New expandable hydrogel-platinum coil hybrid device for aneurysm embolization. Am J Neuroradiol **23**: 1580-1588.

Killer M, Richling B, Minnich B, Lametschwandtner A, Plenk H, Jr. (2004) Unexpected Tissue Engineering: Cartilage neoformation in long-term HydroCoil®-occluded experimental aneurysms. Eur Cell Mater **7, Suppl 2**: 43.

Kwon OK, Han MH, Oh CW, Park IA, Choe G, Lee KH, Chang KH, Han D (2003) Embolization with autologous fibroblast-attached platinum coils in canine carotid artery aneurysms: histopathological differences from plain coil embolization. Invest Radiol **38**: 281-287.

Lee D, Yuki I, Murayama Y, Chiang A, Nishimura I, Vinters HV, Wang CJ, Nien YL, Ishil A, Wu BM, Vinuela F (2007) Thrombus organization and healing in the swine experimental aneurysm model. Part I. A histological and molecular analysis. J Neurosurg **107**: 94-108.

Linfante I, Akkawi NM, Perlow A, Andreone V, Wakhloo AK (2005) Polyglycolide/polylactide-coated platinum coils for patients with ruptured and unruptured cerebral aneurysms: a single-center experience. Stroke **36**: 1948-1953.

Luo G, Ducy P, McKee MD, Pinero GJ, Loyer E, Behringer RR, Karsenty G (1997) Spontaneous calcification of arteries and cartilage in mice lacking matrix GLA protein. Nature **386**: 78-81.

Marlovits S, Tichy B, Truppe M, Gruber D, Vecsei V (2003) Chondrogenesis of aged human articular cartilage in a scaffold-free bioreactor. Tissue Eng **9**: 1215-1226.

Mawad ME, Mawad JK, Cartwright J, Jr., Gokaslan Z (1995) Long-term histopathologic changes in canine aneurysms embolized with Guglielmi detachable coils. Am J Neuroradiol **16**: 7-13.

Molyneux AJ, Kerr RS, Yu LM, Clarke M, Sneade M, Yarnold JA, Sandercock P (2005) International subarachnoid aneurysm trial (ISAT) of neurosurgical clipping versus endovascular coiling in 2143 patients with ruptured intracranial aneurysms: a randomised comparison of effects on survival, dependency, seizures, rebleeding, subgroups, and aneurysm occlusion. Lancet **366**: 809-817.

Murayama Y, Tateshima S, Gonzalez NR, Vinuela F (2003) Matrix and bioabsorbable polymeric coils accelerate healing of intracranial aneurysms: long-term experimental study. Stroke **34**: 2031-2037.

Murayama Y, Vinuela F, Suzuki Y, Do HM, Massoud TF, Guglielmi G, Ji C, Iwaki M, Kusakabe M, Kamio M, Abe T (1997) Ion implantation and protein coating of detachable coils for endovascular treatment of cerebral aneurysms: concepts and preliminary results in swine models. Neurosurgery **40**: 1233-1243; discussion 1244.

Pile-Spellman J, Wu J (1997) Coil embolization of aneurysms: angiographic and histologic changes. Am J Neuroradiol **18**: 43-44.

Plenk H, Jr. (1986) The microscopic evaluation of hard tissue implants. In Williams DF, ed. Techniques of Biocompatibility Testing. Boca Raton, FL, CRC Press, 35-81.

Qiao JH, Fishbein MC, Demer LL, Lusis AJ (1995) Genetic determination of cartilaginous metaplasia in mouse aorta. Arterioscler Thromb Vasc Biol **15**: 2265-2272.

Reul J, Weis J, Spetzger U, Konert T, Fricke C, Thron A (1997) Long-term angiographic and histopathologic findings in experimental aneurysms of the carotid bifurcation embolized with platinum and tungsten coils. Am J Neuroradiol **18**: 35-42.

Rice MA, Anseth KS (2004) Encapsulating chondrocytes in copolymer gels: bimodal degradation kinetics influence cell phenotype and extracellular matrix development. J Biomed Mater Res A **70**: 560-568.

Schulick AH, Taylor AJ, Zuo W, Qiu CB, Dong G, Woodward RN, Agah R, Roberts AB, Virmani R, Dichek DA (1998) Overexpression of transforming growth factor beta1 in arterial endothelium causes hyperplasia, apoptosis, and cartilaginous metaplasia. Proc Natl Acad Sci U S A **95**: 6983-6988.

Seemayer TA, Thelmo WL, Morin J (1973) Cartilaginous transformation of the aortic valve. Am J Clin Pathol **60**: 616-620.

Sherif C, Plenk H, Jr., Grossschmidt K, Kanz F, Bavinzski G (2006) Computer-assisted quantification of occlusion and coil densities on angiographic and histological images of experimental aneurysms. Neurosurgery **58**: 559-566; discussion 566.

Tenjin H, Fushiki S, Nakahara Y, Masaki H, Matsuo T, Johnson CM, Ueda S (1995) Effect of Guglielmi detachable coils on experimental carotid artery aneurysms in primates. Stroke **26**: 2075-2080.

Van Aken PJ, Emeis JJ (1983) Organization of experimentally induced arterial thrombosis in rats from two weeks until ten months. The development of an arteriosclerotic lesion and the occurrence of rethrombosis. Artery **11**: 384-399.

Van Aken PJ, Emeis JJ (1982) Organization of experimentally induced arterial thrombosis in rats: the first six days. Artery **11**: 156-173.

Waldman SD, Couto DC, Grynpas MD, Pilliar RM, Kandel RA (2007) Multi-axial mechanical stimulation of tissue engineered cartilage: review. Eur Cell Mater **13**: 66-75.

Watson KE, Bostrom K, Ravindranath R, Lam T, Norton B, Demer LL (1994) TGF-beta 1 and 25-hydroxycholesterol stimulate osteoblast-like vascular cells to calcify. J Clin Invest **93**: 2106-2113.

Discussion with Reviewers:

Reviewer III: Since the authors have not performed topographical or chemical surface analyses of the implants tested, and it is well known that these affect the biological response, e.g. the surface can be decisive for 1) whether tissue adheres or not, 2) whether a fibrous capsule or inflammation occurs or not, and 3) whether it can encourage or discourage bone formation. Could it be that any changes seen are due to simple surface differences?
Authors: With regard to surface topography, the platinum-tungsten wires for the coils are drawn, and thus have a machined surface, or they are covered by a hydrogel or a resorbable polymer coating. In the swollen state, all the used hydrogels have micro- to macroporous surfaces, into which cells can migrate and differentiate, as can be seen in the figures of our paper. Cartilage and/or bone was not only found adjacent and between coils within the aneurysm sacs and under the new vessel walls, but also in direct contact with both, the hydrogel and platinum surfaces, despite a more pronounced foreign body response to platinum coils. The hydrogels, the resorbable polymer and the platinum coils were only tested for blood compatibility according to ISO 10993, in order to get FDA approval for blood contacting implants. No further chemical or physico-chemical surface characterizations have been performed. However, it should be emphasized that ectopic cartilage or bone formation was so far not expected or intended in thrombus organization after coil embolization of aneurysms, but was an incidental observation. These tissue metaplasias in experimental aneurysms are apparently more related to animal species and the mechanobiology during long-term fibro-vascular healing, than to different coil material properties or surfaces. Since these metaplasias seem to occur also in coil-embolized human intracranial aneurysms, the significance of these new observations for long-term occlusion has to be further investigated.